sellations would be handled more easily, but even binary layers based on the homogeneous circle packings recently studied (Fischer, 1968) could be derived by an extension of this method.

The author is greatly indebted to Dr A. L. Loeb for kindly revising the manuscript and making suggestions that improved the English, and to Professor M. J. Buerger for making his manuscript available prior to publication. Thanks are also due to Drs J. Lima-de-Faria and A. Lopes-Vieira for helpful discussions and encouragement throughout this work. The financial support of the Calouste Gulbenkian Foundation is gratefully acknowledged.

References

BECK, P. A. (1967). *Z. Kristallogr.* **124**, 101–114.
BECK, P. A. (1968). *Acta Cryst.* B**24**, 1477–1481.
BUERGER, M. J. (1947). *J. Chem. Phys.* **15**, 1–16.
BUERGER, M. J. (1967). Private communication.
BURZLAFF, H., FISCHER, W. & HELLNER, E. (1968). *Acta Cryst.* A**24**, 57–67.
COXETER, H. S. M. (1961). *Introduction to Geometry*, pp. 52, 53. New York: Wiley.
FISCHER, W. (1968). *Acta Cryst.* A**24**, 67–81.
GEHMAN, W. G. (1963). *J. Chem. Educ.* **40**, 54–60.
IIDA, S. (1957). *J. Phys. Soc. Japan*, **12**, 222–233.
International Tables for X-Ray Crystallography (1952). Vol. I. Birmingham: Kynoch Press.
LAVES, F. (1956). *Theory of Alloy Phases*, p. 126. American Society of Metals Symposium.
LE CORBEILLER, P. & LOEB, A. L. (1967). TR-47a, Ledgemont Lab., Kennecott Copper Corp., Lexington, Mass. U.S.A.
LIMA-DE-FARIA, J. (1965). *Z. Kristallogr.* **122**, 359–374.
LIMA-DE-FARIA, J. & FIGUEIREDO, M. O. (1969). *Z. Kristallogr.* **130**, 54–67.
LOEB, A. L. (1962). *Acta Cryst.* **15**, 219–226.
LOEB, A. L. (1964). *Acta Cryst.* **17**, 179–182.
LOEB, A. L. (1967). TR-133, Ledgemont Lab., Kennecott Copper Corp., Lexington, Mass. U.S.A.
LOEB, A. L. (1968). TM-18, Ledgemont Lab., Kennecott Copper Corp., Lexington, Mass. U.S.A.
LOEB, A. L. (1970). *J. Solid State Chem.* **1**, 237–267.
MORRIS, I. L. & LOEB, A. L. (1960). *Acta Cryst.* **13**, 434–443.
SMIRNOVA, N. L. (1956). *Kristallografiya*, **1**, 165–170.
TAKEDA, H. & DONNAY, J. D. H. (1965). *Acta Cryst.* **19**, 474–476.
WELLS, A. F. (1954). *Acta Cryst.* **7**, 535–544.
WELLS, A. F. (1968). *Acta Cryst.* B**24**, 50–57.

Acta Cryst. (1973). A**29**, 243

Relations between the DO_9 (ReO_3) Structure Type and Some 'Bronze' and 'Tunnel' Structures

BY B. G. HYDE

School of Chemistry, University of Western Australia, Nedlands, W. A. 6009, *Australia*

AND M. O'KEEFFE

Chemistry Department, Arizona State University, Tempe, Arizona 85281, *U.S.A.*

(*Received* 9 *November* 1972; *accepted* 14 *December* 1972)

A number of the 'bronze' and 'tunnel' structures are derived from the DO_9 type by a simple geometrical operation: examples given are the tetragonal tungsten bronze and related structures, and Mo_5O_{14} and $LiNb_6O_{15}F$. They are seen to form families of crystallographic shear structures of a new type.

Introduction

In the DO_9/ReO_9 structure type [MO_6] octahedra are united by common vertices [Fig. 1(*a*)]. Projection down one of the cubic axes [Fig. 1(*b*)] emphasizes the empty 'tunnels' of square cross-section within the structure. (They are in fact strings of cuboctahedra sharing square faces.) In the $E2_1$/perovskite structure type sites at $\frac{1}{2}\frac{1}{2}\frac{1}{2}$ (cuboctahedra centres), which are empty in DO_9, are occupied by the A cations, *e.g.* by Ca in $CaTiO_3$ [Fig. 1(*c*)]. In some tungsten bronzes A_xWO_3 these same sites are fractionally occupied by alkali metal or other cations.

But there are other bronze structures which also contain sites of high coordination number partly occupied by A cations. One is the tetragonal tungsten bronze (TTB) structure in which these sites are in pentagonal as well as square tunnels in an array of corner-connected [WO_6] octahedra (Magnéli, 1949*a*). Examples of TTB-related structures are legion, particularly in the system $Nb_2O_5+WO_3$ (Stephenson, 1968). A number of binary, ternary and quaternary oxides and oxide-fluorides have related structures but definite stoichiometries: Mo_5O_{14} (Kihlborg, 1963), Ta_3O_7F (Jahnberg & Andersson, 1967) and the closely similar $LiNb_6O_{15}F$ (Lundberg, 1965), and $NaNb_6O_{15}F$ (and $NaNb_6O_{15}OH$)

(Andersson, 1965). In these a tunnel is either completely filled or completely empty: filled pentagonal tunnels contain rows of alternate metal and oxygen atoms/ions, ...MOMO..., the metal coordination polyhedron being a pentagonal bipyramid, $[MO_7]$. (In $NaNb_6O_{15}F$ and $NaNb_6O_{15}OH$ some are filled with Na.)

All these complex 'bronze' and 'tunnel' structures contain a network of corner-sharing $[MX_6]$ octahedra which we will term the *framework*. Elements of DO_9 topology (with square, or distorted-square tunnels) are clearly recognizable, but they are connected in ways which also produce triangular and pentagonal, and sometimes hexagonal, tunnels. The structural relations involved have puzzled crystal chemists for some years (Magnéli, 1949*b*; Wadsley, 1963; Ekström & Nygren, 1972).

Structural relations

In all cases the stoichiometry of the framework is MX_3 as in DO_9 and, in fact, they *can* be geometrically derived from this prototype, sometimes in more than one way. Here we will consider the structures mentioned above, all but one of whose frameworks may be produced from DO_9 by the same simple, novel operation. The same operation can also produce frameworks as yet unknown. The complete structures are obtained by filling a proportion of the tunnels with alkali metal atoms and/or ...MOMO... rows. All except TTB contain the so-called 'pentagonal column': an $[MX_7]$ pentagonal bypyramid joined by its equatorial edges to five $[MX_6]$ octahedra, the M_6X_{27} groups thus formed being linked by corner sharing in a direction normal to the equatorial plane (see, for example, Lundberg, 1971) so that the column stoichiometry is M_6X_{21}.*

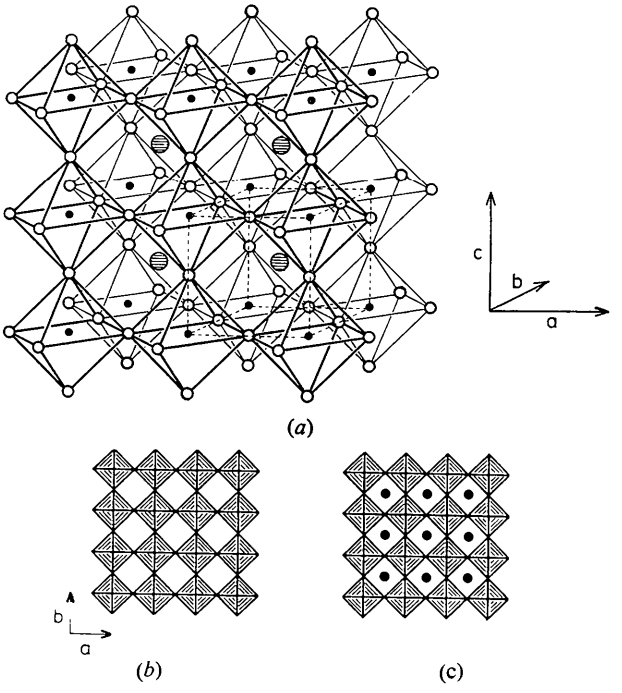

Fig. 1. The ReO_3 (*a*,*b*) and perovskite (*c*) structure types. (*a*) Filled circles, B(Re) cations; open circles, anions; hatched circles, A cation sites, unoccupied in ReO_3, occupied in perovskite. The broken lines outline one unit cell. In (*b*) and (*c*) the two structure types are represented as $[MO_6]$ octahedra and projected along $[00\bar{1}]$.

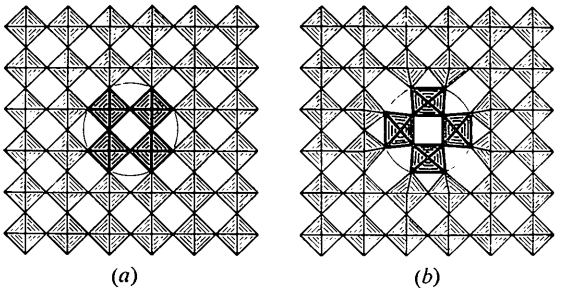

Fig. 2. The ideal, basic, rotation operation which produces pentagonal and triangular tunnels [in (*b*)] from the ReO_3 structure type [in (*a*)]. The group of four heavily outlined octahedra is rotated by $\pi/4$ radians. Projection as in Fig. 1.

Idealized, the basic operation is shown in Fig. 2. Starting with the usual projection of DO_9, a square group of four corner-sharing octahedra (a projected column) is rotated through $\pi/4$ radians. This changes the eight square tunnels peripheral to the rotated group to four triangular and four pentagonal tunnels.† In fact, the shifts of the anions at the periphery of the group are anion–anion vectors, and so it is not necessary to move them. We need only rotate four anion rows (the inner square tunnel centred on the rotation axis) and the four adjacent ...MXMX... rows. Together these form one column of DO_9 'unit cells'. The resulting 'defect' may be described as a cylindrical rotation fault (Bursill & Hyde, 1972*a*), *rotary stacking fault* or cylindrical antiphase boundary (CAPB).‡ Neither the stoichiometry nor the number of anion–anion contacts is changed by the operation.

The frameworks of the complex structures are derived from DO_9 by regular repetition of this operation. In all the resulting structures at least one of the pentagonal

* Two other structures, those of $W_{18}O_{49}$ (Magnéli, 1949*c*) and $Mo_{17}O_{47}$ (Kihlborg, 1960) are usually grouped with the ones discussed here. They also contain pentagonal columns, but cannot be derived from DO_9 in the same way, and will be considered elsewhere.

† Of course, four octahedra could combine with the four triangles to produce four pentagonal bipyramids. But this would result in increased edge-sharing between coordination polyhedra, *cf.* below and Magnéli (1949*d*).

‡ The term 'antiphase boundary' (APB) has previously implied a *translational* fault: across the boundary the structure is displaced by a vector $\mathbf{R}=\frac{1}{2}[l\mathbf{a},m\mathbf{b},n\mathbf{c}]$, where **a**, **b** and **c** are lattice (translation) vectors, and at least some of l,m,n are integers, and some may be zero. By analogy, across a CAPB the structure is displaced by a rotation pseudovector $\boldsymbol{\omega}$, where $2\boldsymbol{\omega}$ is a lattice pseudovector (Bursill & Hyde, 1972*a*). In the present instance $\omega=\pi/4$ rad: $2\omega=\pi/2$ rad since, in the framework, the rotation axis is a fourfold symmetry axis.

tunnels in each fault will be occupied by interpolated atoms and, presumably, the fault is generated because these additional atoms are too large for the square tunnels in DO_9. The operation reduces the repulsion part of the crystal energy by enlarging the occupied tunnel.

Different frameworks are produced by varying the ordered array of rotation axes on a two-dimensional superlattice of DO_9.* If they are spaced sufficiently far apart the outcome is obvious. If not, the various spacings employed in Fig. 3 produce further modifications in the topology of the net of corner-connected octahedra. When the vector between rotation centres is ⟨220⟩, instead of eight pentagonal tunnels we get six pentagonal tunnels, plus one hexagonal tunnel between the rotation groups. When the vector is ⟨210⟩ we again get six pentagonal tunnels but now, instead of eight triangular tunnels we get 6 triangular plus two quadrilateral (distorted-square) tunnels. When the vector is ⟨200⟩ we get four pentagonal, six triangular and two hexagonal tunnels; the two rotation groups are united by a common octahedral edge. (A simple systematic way of showing this is as follows. In Fig. 2(*b*) put a minus sign in each triangle and a plus sign in each pentagon. These represent respectively the loss and gain of a corner by the original peripheral squares [Fig. 2(*a*)] during the operation. The operation Fig. 3(*a*) → (*b*) gives + + = +2 at the centre of *b*, *i.e.* 4-gon → 6-gon: Fig. 3(*c*) → (*d*) gives + − = 0 in the two quadrilateral tunnels in *d*: Fig. 3(*e*) → (*f*) gives − − = −2 at the centre of *f*, *i.e.* 4-gon → 2-gon = a line; and + + = +2, *i.e.* 4-gons → 6-gons, to the left and right.)

* A three-dimensional array is clearly possible, at least in principle.

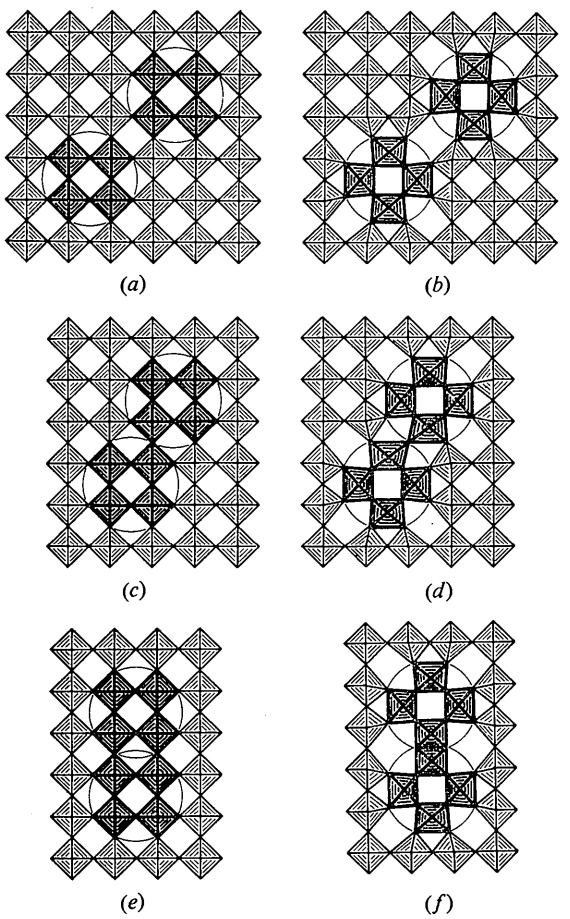

Fig. 3. Special cases of closely spaced pairs of rotation centres: (*a*) → (*b*), separation between centres = ⟨220⟩, giving a hexagonal tunnel at the centre of (*b*); (*c*) → (*d*), separation = ⟨210⟩, two quadrilateral tunnels produced at the centre of (*d*); (*e*) → (*f*), separation = ⟨200⟩, a pair of edge-shared octahedra produced at the centre of (*f*).

In a given framework, variation in the arrangement and/or the proportion of filled tunnels yields additional superstructure possibilities (*cf.* TTB and $Nb_{16}W_{18}O_{94}$ below.)

Fig. 4 depicts the production of the TTB framework from DO_9. The maximum value of x in A_xWO_3 is obviously [Fig. 4(*a*)] $x = 0{\cdot}6$. [The TTB pseudocell in Fig. 4(*a*) contains ten square tunnels. After the rotation Fig. 4(*a*) → (*b*), four of these become triangular (and are then, presumably, too small to accommodate interpolated alkali metal atoms). These are devoid of an open circle in Fig. 4(*a*). The maximum cell content therefore changes from a possible $A_{10}W_{10}O_{30}$ in the perovskite type, Fig. 4(*a*), to $A_{10-4}W_{10}O_{30} = A_6W_{10}O_{30}$ in Fig. 4(*b*); *i.e.* $AWO_3 \rightarrow A_{0{\cdot}6}WO_3$.] In the idealized structure [Fig. 4(*b*)] the tetragonal unit cell has $\mathbf{a} = -\mathbf{a}_R - 3\mathbf{b}_R$, $\mathbf{b} = 3\mathbf{a}_R - \mathbf{b}_R$ and $\mathbf{c} = \mathbf{c}_R$.* The actual TTB structure [Fig. 4(*c*)] is topologically identical with the ideal. All pentagonal and square tunnels are fractionally occupied for $x < 0{\cdot}6$.

In Fig. 5 the structure of $Nb_{16}W_{18}O_{94}$ (= $8Nb_2O_5.18WO_3$) (Sleight, 1966), one of many mixed Nb(V) + W(VI) oxides with structures based on the TTB framework, is similarly derived. The ideal structure has $\mathbf{a} = -\mathbf{a}_R - 3\mathbf{b}_R$, $\mathbf{b} = 3(3\mathbf{a}_R - \mathbf{b}_R)$ and $\mathbf{c} = \mathbf{c}_R$. Again the ideal and real structures [Figs. 5(*b*) and (*c*)] are topologically identical. One rotation group (at the centre of the cell) has two of its four pentagonal tunnels filled. In the others only one of the four pentagonal tunnels is occupied.

The structure given for $3Bi_2O_3.\ 17Nb_2O_5 = Bi_6Nb_{34}O_{94}$ (Keve & Skapski, 1968) is derived from that of $Nb_{16}W_{18}O_{94}$ [$= (Nb, W)_{34}O_{94}$] by interpolating Bi atoms into the empty pentagonal and some of the empty distorted square tunnels in Fig. 5(*b*) or (*c*).

Fig. 6 shows how the MoO_3 framework (not, of course the MoO_3-structure type) of Mo_5O_{14} may be derived from DO_9. The idealized tetragonal unit cell, $Mo_{160}O_{448}$, has $\mathbf{a} = 12\mathbf{a}_R$, $\mathbf{b} = 12\mathbf{b}_R$ and $\mathbf{c} = \mathbf{c}_R$. The diagram shows the commonly used subcell with $\mathbf{a}' = \mathbf{a}/2$.

* The subscript R denotes indices based on the DO_9/ReO_3 subcell.

The doubling arises from a slight puckering of the Mo nets parallel to the (001) plane. The rotation groups are arranged in isolated pairs as in Fig. 3(*a*), with two mutually perpendicular orientations. Consequently there are hexagonal and pentagonal tunnels. Only one pentagonal tunnel in each rotation group in the framework is occupied. [This has the interesting consequence that in each subcell there are two groups of four octahedra, at the 0,0 and $\frac{1}{2},\frac{1}{2}$ positions, rotated with respect to surrounding octahedra as in Fig. 2(*b*); but the arrangement is not supported by any of the peripheral pentagonal tunnels being occupied by interpolated atoms. If some or all of these groups (there are eight of them in the full unit cell) were also rotated by $\pi/4$ radians a sequence of polymorphs would arise.]

In Fig. 7 the frameworks of Ta_3O_7F and $LiNb_6O_{15}F$ are derived from DO_9. The rotation groups are now arrayed in continous slabs parallel to $[1\bar{2}0]_R$, connected as in Fig. 3(*b*), and separated by unchanged slabs of DO_9. The new unit cell axes are $\mathbf{a}=4\mathbf{a}_R-2\mathbf{b}_R$, $\mathbf{b}=\mathbf{c}_R$ and $\mathbf{c}=-\mathbf{a}_R-2\mathbf{b}_R$.

The Ta_3O_7F and $LiNb_6O_{15}F$ structures are composed entirely of corner-connected 'pentagonal columns'. [In the latter Li atoms are interpolated into the Ta_3O_7F structure type, but their positions are not known (Lundberg, 1965).] The structure of $NaNb_6O_{15}F$ (and $NaNb_6O_{15}OH$) is very similar (Fig. 8). It also contains

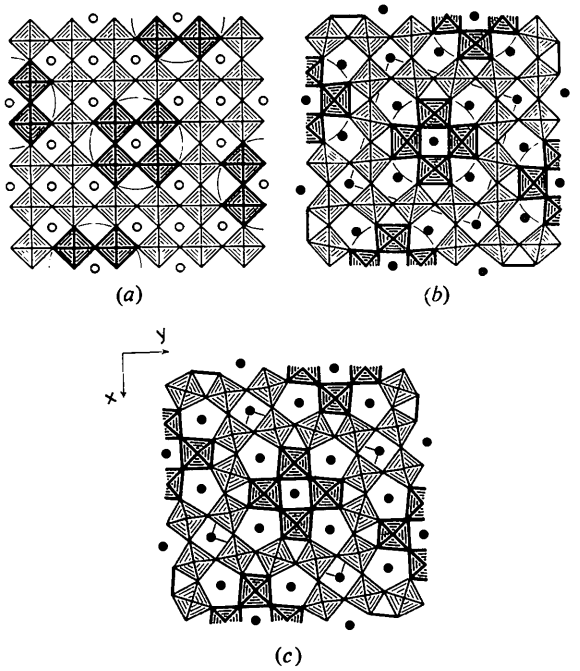

Fig. 4. Production of the TTB structure from DO_9. (*a*) DO_9 with groups to be rotated heavily outlined, and sites to be fractionally occupied by alkali metal atoms shown as open circles. (*b*) After rotation according to Fig. 2, and filling of A sites. (*c*) The real tetragonal potassium tungsten bronze structure. It is apparent that (*b*) and (*c*) are topologically identical.

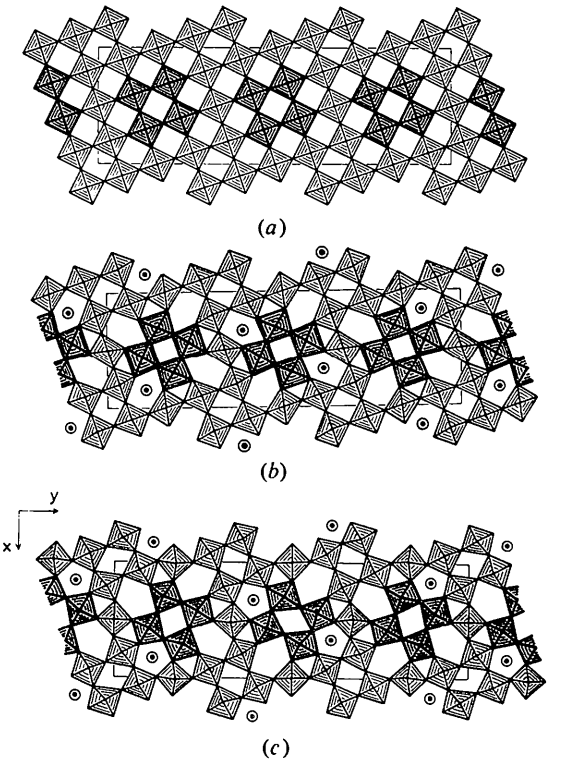

Fig. 5. Derivation of the structure of $N_{16}W_{18}O_{94}$ from the DO_9 type. In (*a*) are indicated the new unit cell (3 TTB subcells) and the groups to be rotated. (*b*) shows the ideal structure after the rotations and filling some of the pentagonal tunnels with ...MOMO... rows. Small filled circles are metal atoms, larger open circles are oxygens. These metals are in pentagonal bipyramidal, $[MO_7]$, coordination. (*c*) gives the real structure. All are projected along $[00\bar{1}]$.

only corner-connected 'pentagonal columns' but the way in which they are connected produces pentagonal tunnels which are occupied by Na. A comparison of the two structures ($MNb_6O_{15}F$, M = Li, Na) shows that they both consist of identical slabs of pentagonal columns of single width [parallel to the *c* axis in Fig. 7(*c*)]: in $LiNb_6O_{15}F$ the orientation of the columns differs by $\pi/5$ radians between adjacent slabs: in $NaNb_6O_{15}F$ they do not differ.

Hence, formally, each structure can be converted to the other by rotating each column in alternate slabs by $\pi/5$ radians. Starting with $LiNb_6O_{15}F$ (and ignoring the Li) this converts one third of the quadrilateral tunnels to pentagonal tunnels and another third to triangular tunnels – the $NaNb_6O_{15}F$ arrangement. This is a rotation operation involving a larger unit: the vectors between rotation centres are: $LiNb_6O_{15}F$, $[10\bar{1}]$ and [001]; $NaNb_6O_{15}F$, $\frac{1}{2}[011]$ and $[01\bar{1}]$ or $\frac{1}{2}[0\bar{1}1]$ and [011].[*N.B.* the rotation of a still larger 'hexagonal' column by $\pi/9$ radians relates the hexagonal tungsten bronze structure to that of $K_2W_4O_{13}$ (Bursill & Hyde, 1972*a*).] Alternatively, the $Nb_6O_{15}F$ structure of the Li compound may be regarded as that of the Na compound multiply twin-

ned by a rotation of π about the normal to (001), the composition plane being (011).

Discussion

It has previously been pointed out that a crystallographic shear (CS) plane may be regarded as an APB plane plus interpolated 'interstitial' cations (in rutile-related structures) (Bursill, Hyde & O'Keeffe, 1972; Bursill & Hyde, 1972*b*) or ...MOMO... rows (in DO_9-related structures) (Bursill & Hyde, 1972*c*). The APB component reduces respectively the amount of face-sharing (Bursill *et al.*, 1972) or edge-sharing (Magnéli, 1949*d*) between [MO_6] octahedra and, presumably, the energy of the crystals. The frameworks described here contain CAPB's, and hence the tunnel structures generated from them by interpolation of ...MXMX... rows may also be regarded as CS structures, but with cylindrical (rotational) rather than planar (translational) CS surfaces.

The possibilities for disorder, intergrowth and non-

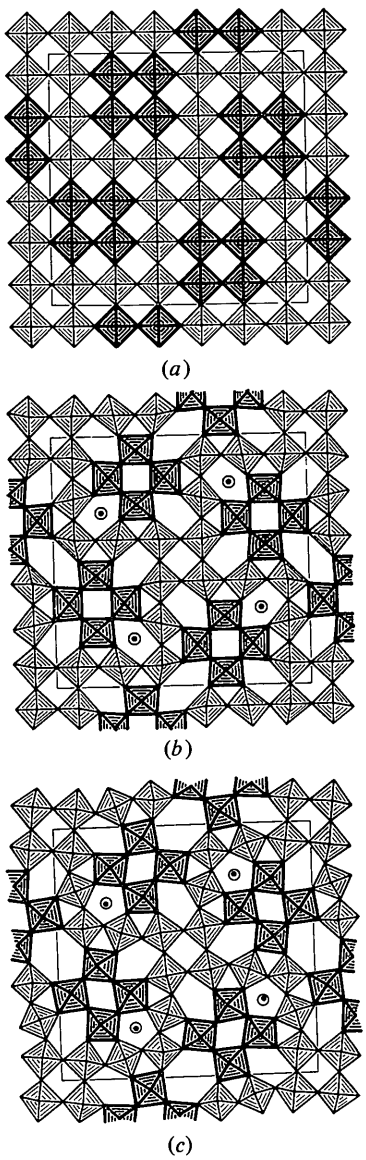

Fig. 6. Production of the Mo_5O_{14} type from DO_9: (*a*) before, and (*b*) after rotating the appropriate groups of octahedra, and filling some of the pentagonal tunnels with ...MOMO... rows. (*c*) shows the real structure. The tetragonal subcell outlined has $\mathbf{a}'=\mathbf{a}/2$. Note (i) that either or both the groups of four octahedra at the centre and origin of the subcell may, in principle, also be rotated by $\pi/4$ radians, since their peripheral pentagonal tunnels are all empty; (ii) the hexagonal tunnels at the subcell face centres [*cf.* Fig. 3(*b*)].

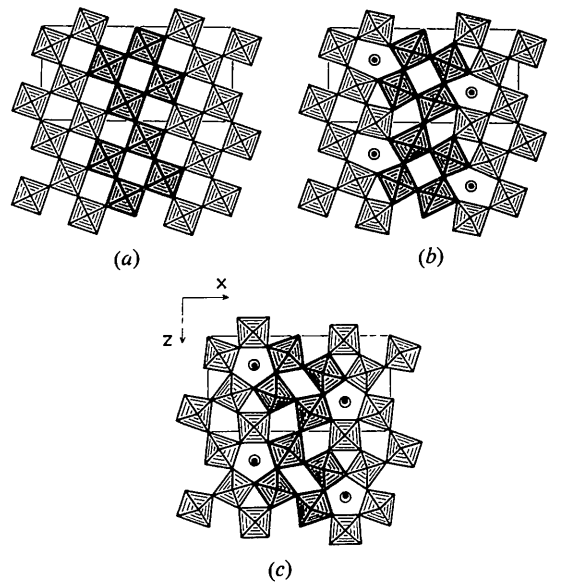

Fig. 7. Production of the Ta_3O_7F and $LiNb_6O_{15}F$ structures from DO_9. (*a*) Before, and (*b*) after the rotation of the groups and filling of some of the pentagonal tunnels [*cf.* Fig. 3(*d*)]. (*c*) shows the real structure of $LiNb_6O_{15}F$, although the Li positions are not located.

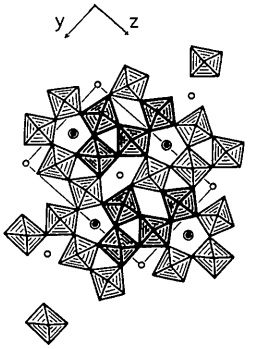

Fig. 8. The real structure of $NaNb_6O_{15}F$ (Small open circles = Na). Compare with Fig. 7(*c*), and note that in going from Fig. 7(*d*) to Fig. 8 the pentagonal columns on the right have been rotated clockwise by $\pi/5$ radians. Otherwise there is a one-to-one correspondence between all the [MX_6] octahedra and [MX_7] pentagonal bipyramids in both drawings.

stoichiometry are obvious (see, for example, Allpress, 1972).

We are grateful to Docent Sten Andersson for bringing the Keve & Skapski reference to our attention, and wish to acknowledge support from the U.S. Air Force Office of Scientific Research (Grant No. AFOSR-72-2312), the Australian Research Grants Committee and the National Science Foundation.

References

ALLPRESS, J. G. (1972). N.B.S. Special Publication 364, *Solid State Chemistry*, pp. 104–109. Proceedings of 5th Materials Research Symposium; edited by R. S. ROTH and S. J. SCHNEIDER JR. Washington: U.S. Government Printing Office.

ANDERSSON, S. (1965). *Acta Chem. Scand.* **19**, 2285–2290.

BURSILL, L. A. & HYDE, B. G. (1972*a*). *Nature Phys. Sci., Lond.* **240**, 122–124.

BURSILL, L. A. & HYDE, B. G. (1972*b*). *Progr. Solid State Chem.* **7**, 177–253.

BURSILL, L. A. & HYDE, B. G. (1972*c*). *J. Solid State Chem.* **4**, 430–446.

BURSILL, L. A., HYDE, B. G. & O'KEEFFE, M. (1972). N.B.S. Special Publication 364, *Solid State Chemistry*, pp. 197–204. Proceedings of 5th Materials Research Symposium; edited by R. S. ROTH and S. J. SCHNEIDER JR. Washington: U.S. Government Printing Office.

EKSTRÖM, T. & NYGREN, M. (1972). *Acta Chem. Scand.* **26**, 1827–1835.

JAHNBERG, L. & ANDERSSON, S. (1967). *Acta Chem. Scand.* **21**, 615–619.

KEVE, E. T. & SKAPSKI, A. C. (1968). *Nature, Lond.* **217**, 841.

KIHLBORG, L. (1960). *Acta Chem. Scand.* **14**, 1612–1622.

KIHLBORG, L. (1963). *Ark. Kemi*, **21**, 427–436.

LUNDBERG, M. (1965). *Acta Chem. Scand.* **19**, 2274–2284.

LUNDBERG, M. (1971). *Univ. Stockholm Chem. Commun.* No. **XII**, 21.

MAGNÉLI, A. (1949*a*). *Ark. Kemi*, **1**, 213–221.

MAGNÉLI, A. (1949*b*). *Ark. Kemi*, **1**, 227.

MAGNÉLI, A. (1949*c*). *Ark. Kemi*, **1**, 223–230.

MAGNÉLI, A. (1949*d*). *Ark. Kemi*, **1**, 513.

SLEIGHT, A. W. (1966). *Acta Chem. Scand.* **20**, 1102–1112.

STEPHENSON, N. C. (1968). *Acta Cryst.* B**24**, 637–653.

WADSLEY, A. D. (1963). *Non-stoichiometric Compounds*, p. 129, edited by L. MANDELCORN. New York: Academic Press.

Acta Cryst. (1973). A**29**, 248

Temperature Dependence of Integrated Thermal Diffuse Scattering

BY JOHN S. REID

Department of Natural Philosophy, The University, Aberdeen AB9 2UE, Scotland

(*Received* 9 *November* 1972; *accepted* 28 *November* 1972)

The temperature dependence of the integrated thermal diffuse scattering (T.D.S.) surrounding Bragg reflexions is discussed, with particular reference to cryogenic applications. Detailed calculations of the T.D.S. and its ratio to the Bragg intensity are presented for NaCl over the range 0 to 800°K. The T.D.S. includes not only the one-phonon contribution but also multiphonon processes. The temperature dependence of the T.D.S.-to-Bragg ratio is shown to fall off more quickly at low temperatures than the Debye–Waller exponent values. Some insight is gained into the importance of multiphonon processes, and it is concluded that there is much to be gained both in the reduction of T.D.S. and in the increase in intensity of higher-order reflexions by cooling to liquid-nitrogen temperatures.

1. Introduction

There is a growing interest in the application of cryogenic techniques (Coppens, 1972) to cool a single crystal sample which is being studied by X-ray diffraction. Two of the principal reasons for cooling are to increase the intensity of the weaker reflexions and to reduce the thermal diffuse scattering (T.D.S.) corrections which have to be made to all the observed Bragg intensities. These corrections may be large at room temperature but the difficulty of making them for most crystals has led to a lack of confidence in current procedures. In addition, the temperature dependence is considered only in the high-temperature limit (*e.g.* Warren, 1969, Jennings, 1970) and as a result there are no reliable estimates of the reduction in the T.D.S. to be expected on cooling to cryogenic temperatures. Hence in the following paragraphs this temperature dependence is discussed and accurate figures for the dependence of the (integrated) T.D.S. surrounding Bragg peaks are shown for NaCl. This substance has been widely studied by crystallographers and is used here as a test material because good thermal data are available. Its Debye temperature is almost 300°K.

2. The thermal diffuse scattering

The starting point for the calculation is the numerical technique of Reid & Smith (1970*a*) used to find the